Atmosphere Control during Debinding of Powder Injection Molded Parts*

J.A. Moore, B.P. Jarding, B.K. Lograsso, and I.E. Anderson

Atmosphere control during debinding of powder injection molded (PIM) parts is an important parameter to consider. Experimental results have shown that a stagnant atmosphere containing volatiles evolved during debinding can cause slumping of the green samples. Removal of volatiles from the sample zone aids debinding and can reduce cycle times and improve sample quality. Residual carbon and oxygen can be controlled during debinding by adjusting the atmosphere composition. This paper presents the results of PIM 70 vol% spherical copper powder and 30 vol% binder. Debinding atmospheres were altered to determine the effect of debinding on the green body and the sintered sample.

Keywords
debinding, sintering, injection molding

1. Introduction

POWDER injection molding (PIM) allows net shape forming of metal or ceramic powders with significant cost advantages over automated machining for small sized, high volume, high value added parts. The flexibility of injection molding technology was transferred from the plastics industry where complex three-dimensional consumer products have been designed and molded for many years. The advantages of producing complex shapes with close dimensional control, uniform fine-grained microstructures, and high densities fueled the growth of this process. The PIM process involves mixing a metal or ceramic powder with a polymer to allow viscous flow during mixing and molding. The most common binders are thermoplastic hydrocarbons that soften or melt at a modest temperature (50 to 200 °C) enabling mixing and molding. The binder acts as a carrier for the powder particles to provide rheological characteristics that allow viscous flow, typically at temperatures between 50 and 200 °C depending on the polymers used. Upon cooling, the powder and binder mixture maintains its shape allowing extraction of the net shape part from the mold cavity. During subsequent processing, the binder is removed, and the part is sintered into a usable product. Debinding is accomplished by thermal degradation, chemical leaching, wicking, or combinations of these techniques. Thermal degradation is common to all of these methods of binder removal (Ref 1) and is the focus of this investigation.

Thermal debinding is a time consuming operation. Typical powder and binder systems contain 25 to 50 vol% organic binder that must be removed before parts can be sintered. Because of the large quantity of binder in PIM parts, cycle times can be as long as several days, creating a major expense for producers of PIM parts. Carbon and oxygen content in the sintered part is affected by the debinding operation (Ref 2); therefore, control of the furnace atmosphere during the binder removal step is necessary to optimize the final part properties.

The binder removal process progresses through three stages during a typical thermal cycle. The first stage involves thermal expansion of the powder and binder and melting of the binder. Hydraulic pressures develop because of the thermal expansion mismatch between the powder and binder. As long as the compact remains saturated with binder, hydraulic pressures continue to be the dominant force on the compact. These pressures can lead to slumping of the compact and are dependent on the thickness of the part (Ref 3). The binder must be designed to accommodate these pressures, usually by using more than one component with different thermal characteristics. The second stage occurs when increasing temperature causes low molecular weight components to evaporate at the surface. Capillary forces move liquid binder from the center of the compact to the surface where evaporation can continue. Debinding rates must be carefully controlled to prevent initiation of defects, such as cracks and blisters (Ref 3). Eventually the porosity of the compact allows binder evaporation to occur in the interior and escape through the developed interconnected network of porosity. The third and final stage involves thermal decomposition of the remaining binder at higher temperature. High levels of open binder-free porosity at this stage allows faster binder removal rates (Ref 3). Residual carbon is often left in the debound compact, which may be a hindrance to sintering. Removal of the residual carbon can be accomplished during the final stage of debinding by using reactive atmospheres to remove the binder residuals.

Atmosphere control is vital to successful binder removal. Since the initial stages involve evaporation of the binder, there must be some mechanism to remove the evolved vapors from the area near the parts to prevent the binder from recondensing on the part. This occurs if the binder vapors reach a saturation concentration level in the vicinity of the part. Flowing gas is commonly used to transport vapors from the furnace at controlled flow rates. This reduces the partial pressure of binder vapors to prevent saturation and condensation. During the decomposition stage of debinding, the atmosphere in the furnace determines what reactions occur and how much of the carbonaceous residue is removed from the compact. In another study (Ref 4), inert atmospheres controlled the rate of binder removal over a wider temperature range compared with an oxi-

J.A.Moore, B.P. Jarding, B.K. Lograsso, and **I.E. Anderson,** Ames Laboratory, Metallurgy and Ceramics Div., Iowa State University, Ames, IA 50011, USA.

*This paper was originally presented at the symposium "Particulate Materials in Rheological Applications," TMS 1993 Fall meeting, Materials Week Program.

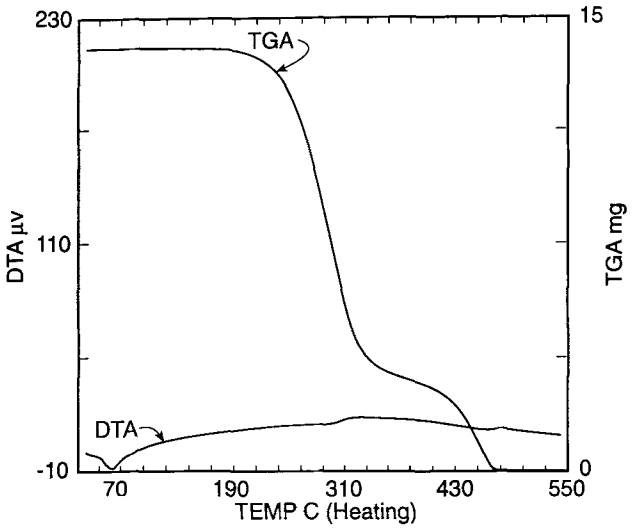

Fig. 1 TGA and DTA plot for binder decomposition in flowing argon. Heating rate of 10 K/min

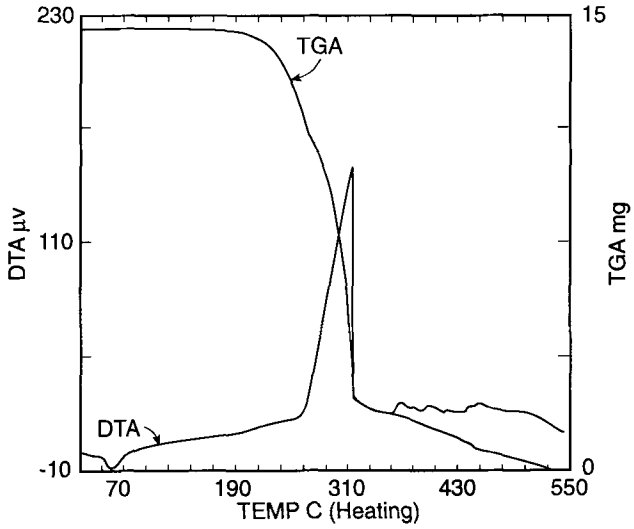

Fig. 2 TGA and DTA plot of binder decomposition in flowing air. Heating rate of 10 K/min

Table 1 Copper powder morphology

Shape	Spherical
Particle size	15 to 45 µm
Theoretical density (pure copper)	8.92 g/cc(a)
Pycnometer density	9.00 g/cc
Impurities being studied	O 130 ppm
(By inert gas fusion)	C 30 ppm

(a) From *CRC Handbook of Chemistry and Physics*, CRC Press, 1989-1990.

dizing atmosphere. This suggests that the debinding atmosphere composition could be adjusted as debinding progresses to optimize the rate of binder removal. However, optimizing the debinding rate was not in the scope of this study.

The purpose of this study was to examine how different atmospheres affect binder removal in copper PIM samples. Complete binder removal is desired, as well as lowering carbon and oxygen impurity levels in the powder used. Inert (argon) atmospheres were used as a baseline to determine the impact that oxidizing (air and O_2/Ar mixture) has on residual carbon and oxygen contents. Additionally, vacuum was used to remove a major portion of the binder during initial stages of debinding, to examine the effect of low partial pressures of oxygen and nitrogen, and to reduce the partial pressure of the binder vapors in the presence of PIM parts.

2. Experimental Procedure

The copper powder used in this investigation was produced by high pressure gas atomization. Powder morphology is summarized in Table 1. Spherical particles sized from 15 to 45 µm were mixed with a three component binder primarily composed of paraffin wax at 100 °C while stirring. The resulting mixture was homogenized with a twin screw extruder at 80 revolutions per minute (rpm) and 75 °C. The final mixture ratio was 70.18 vol% copper and 29.82 vol% binder. This feedstock was molded with a reciprocating screw injection molder to produce 19 mm diameter by 6.4 mm thick samples.

Debinding temperatures were selected by thermogravimetric analysis (TGA) and differential thermal analysis (DTA) measurements performed in flowing argon. The TGA indicated three distinct decomposition steps in the binder (Fig. 1). Furnace profiles were programmed using the decomposition of the first component to leave residual binder for handling the compacts for mass and geometry measurements. TGA and DTA were also done with flowing air to compare the degradation of the binder in an oxidizing atmosphere (Fig. 2). The DTA curve for air debinding shows a sharp exothermic peak indicating rapid decomposition of the binder. The DTA curve for argon exhibits a smooth response to thermal treatment indicating a controlled decomposition reaction. This supports using inert atmospheres to control the rate of binder removal. The TGA plots indicated that complete decomposition of the binder occurred in argon atmosphere at approximately 475 °C; in air atmosphere, it did not occur until approximately 525 °C. This would suggest that the binder reacting with the oxygen or nitrogen in the air atmosphere forms more stable organic compounds, which in turn require higher temperature to decompose. This phenomenon was also observed by Wright et al. (Ref 4).

Temperatures for debinding were determined by selection of temperature ranges on the TGA curves where significant events occurred. Initial set points were selected near the melting point of the paraffin component and held for 4 h at 60°C in order to allow the molded samples expansion to reach thermal equilibrium. Thermal expansion of the unmelted binder components was allowed to equilibrate at 90 °C in the next thermal segment. This was done to remove stresses that may have been molded into the specimen. Temperature was ramped at 5 K/h to 280 °C and held for 2 h before ramping to 350 °C at 100 K/h and

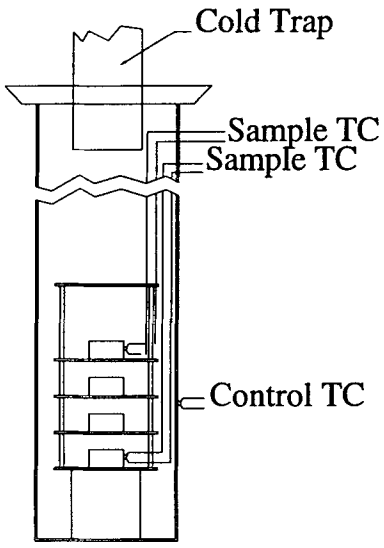

Fig. 3 Schematic of the vertical furnace used for initial binder removal

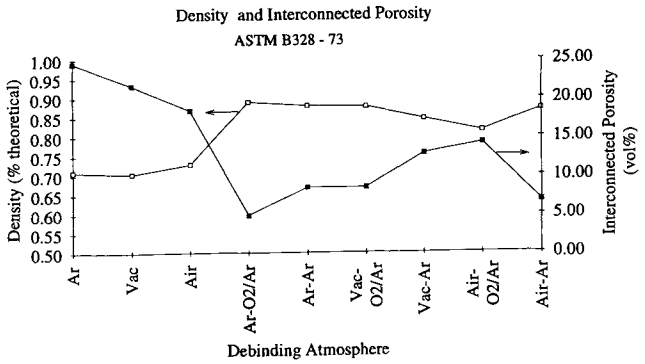

Fig. 5 Plot of density and interconnected porosity of debound and sintered samples

furnace cooling. Sample temperature was recorded to verify the actual processing temperature.

Binder removal was accomplished in two operations. Initial debinding was done in a vertical furnace configuration, shown schematically in Fig. 3. Sample temperatures were recorded for comparison with temperature set points selected. The three atmospheres in Table 2 were selected for initial debinding to determine the effects of atmosphere for removal of the paraffin component. First and second stage debinding mechanisms (thermal expansion, melting and evaporation of the low molecular weight components) are occurring in this operation. These mechanisms are referred to as first stage debinding in the rest of this paper. The same furnace profile was used for all debinding cycles. Mass, dimensional change, interconnected porosity and densities for the PIM disks were recorded.

The remaining binder was decomposed at 700 °C immediately before sintering with either of two atmosphere com positions in a horizontal furnace configuration shown schematically in Fig. 4. Decomposition of the remaining binder will be referred to as final stage debinding in this paper. Control of

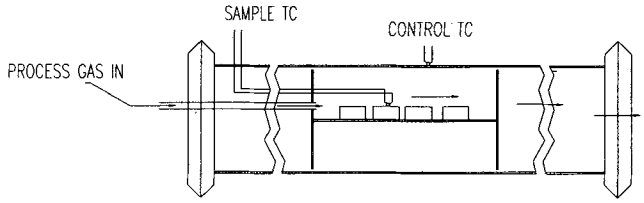

Fig. 4 Horizontal furnace configuration used for final stage debinding and sintering of samples

Table 2 Debinding atmospheres used for paraffin removal

Inert (argon 99.998%)	Flow at 670 cc/min (4 atmosphere changes/h)
Oxidizing (zero grade air)(a)	Flow at 670 cc/min (4 atmosphere changes/h)
Vacuum	5×10^{-5} Torr

(a) Synthetic blend of nitrogen and oxygen, O_2 19.5 to 23.5%.

the residual carbon is accomplished in this phase of debinding. With copper, carbon is not desirable in the final part since excess residual carbon will prevent sintering to high densities. A nonreactive argon atmosphere was compared to an oxidizing atmosphere composed of a mixture of 10 vol% oxygen with the balance argon, which was used to react with the carbon. This atmosphere was measured and mixed with mass flow controllers at 100 mL/min and introduced for 20 min. Preventing oxidation of the compact is necessary because oxidation will increase the volume of the individual particles. This will separate the particles thus limiting the particle to particle contact area, which interferes with sintering. Possible reactions and standard free energy changes are given in Table 3. Formation of CO and CO_2 are favored over the oxidation of the copper, and the ΔG^0 potential is nearly the same for both reactions.

Calculations using 200 mL O_2 reacting with carbon to form CO_2 will consume 0.171 g of carbon, or 0.342 g of carbon if the reaction yields CO. Oxidation of the copper will occur unless the partial pressures of CO and CO_2 are kept well below equilibrium. Flowing gas will keep the partial pressures of CO and CO_2 from reaching equilibrium, maintaining the CO and CO_2 reaction, and limiting the formation of copper oxide. The permeability of the compact with oxygen is also a factor in the ability of gas to penetrate the sample and reach the carbon. Since the compact porosity is open at this point of processing and the temperature is below the temperature where significant sintering is occurring, the carbon should be available to the oxygen for reaction.

Sintering was done at 1000 °C for 1 h in flowing 5 vol% H_2 and 95 vol% He at one liter per min to reduce oxides that may have formed on the compacts during final stage debinding and from the original powder. Helium was selected over argon because of its higher thermal conductivity. Samples were furnace cooled to room temperature before removal from the furnace. Density, interconnected porosity, mass, and final dimensions were recorded. Residual carbon and oxygen were analyzed using inert gas fusion.

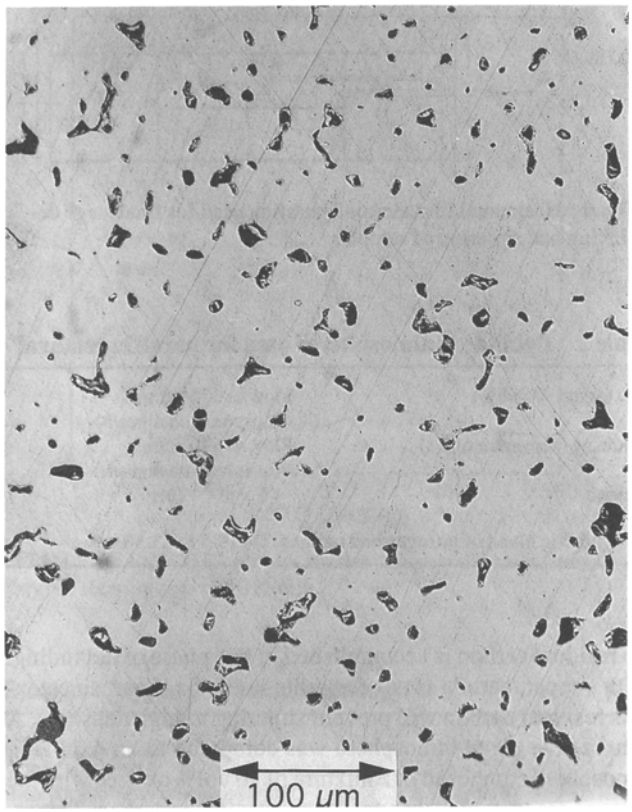

Fig. 6 Sintered microstructure Ar-O_2/Ar debinding atmospheres at the center

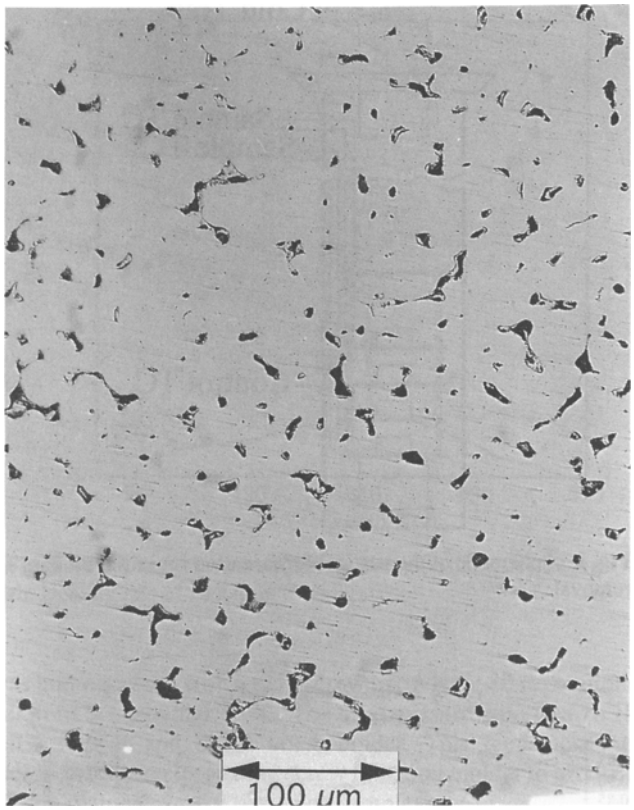

Fig. 7 Sintered microstructure of Ar-Ar debinding atmospheres at the center

Table 3 Standard free energy changes for possible reactions in final binder removal stage

Reaction	ΔG^0 calories
$C(s) + 1/2O_2(g) = CO(g)$	$-26{,}700 - 20.95T$
$C(s) + O_2(g) = CO_2(g)$	$-94{,}200 - 0.2T$
$2Cu(s) + 1/2O_2(g) = Cu_2O(s)$	$-40{,}500 - 3.92T \log T + 20.5T$

From Ref 5.

3. Results

3.1 *First Stage Debinding*

Samples from vacuum debinding showed no change in color and resulted in an average binder loss of 78.8 wt%. In zero grade air, the samples were coated with a black layer, presumably carbon particles condensed on the surface of the sample, with an average binder loss of 34.9 wt%. This binder loss may be somewhat misleading as to the effectiveness of this atmosphere because of the layer of carbon deposited on the surface was removed from the interior. Cracks from 1 to 4 mm developed perpendicular to the edge of these samples. The decomposition reaction with the oxygen in the air may have evolved more gas than could escape, which caused excess pressure to accumulate inside the sample. These cracks were caused as hoop stresses developed. Samples in the argon atmosphere had the highest average binder loss of 91.6 wt%. The samples showed no color change. However 3 of 10 samples showed signs of starting to slump, and 2 of 10 samples slumped.

The data indicated that the temperature from the top to bottom sample varied by approximately 11 °C, and the maximum temperature attained was 346 °C for flowing air and argon while the vacuum process resulted in an average deviation of 6.5 °C from top to bottom sample and a maximum temperature of 328 °C. The sample temperature deviation in the flowing gas atmospheres can be attributed to the introduction of room temperature gas into the furnace. The low maximum temperature of the vacuum debinding run can be attributed to poor convection heating.

The cold trap collected varying amounts of binder vapors. In the vacuum run, the cold trap was coated uniformly with a 3 mm thick layer of white binder residue. Wax vapors condensed on the cold surfaces of the cold trap without decomposition. In the case of flowing argon, the cold trap condensed a very small amount of binder vapor. This condensate was not decomposed, but the quantity indicated that the majority of the binder was carried out with the flowing gas. In the case of the air atmosphere, the cold trap was coated with a layer of brown decomposed binder, and there was an odor of burnt wax indicating that combustion had occurred.

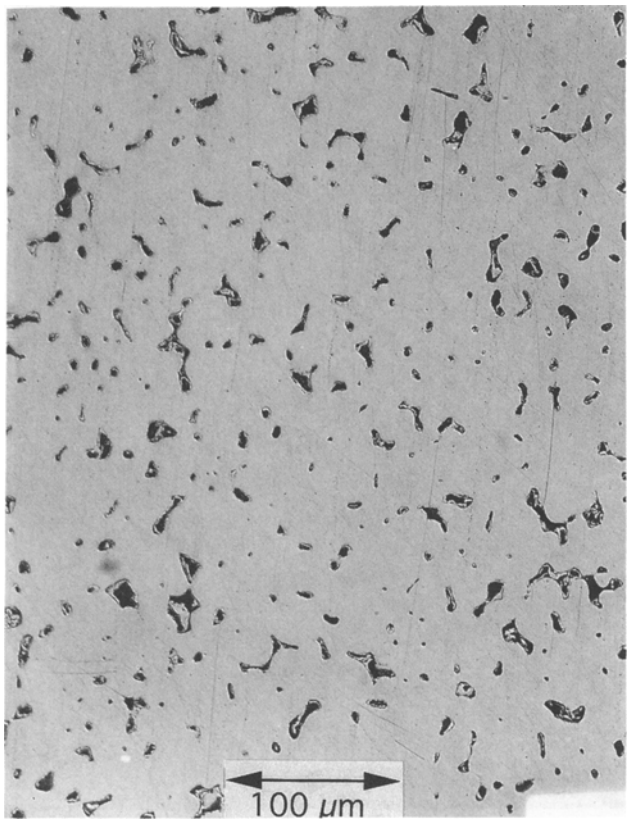

Fig. 8 Sintered microstructure vacuum-O_2/Ar debinding atmospheres at the center

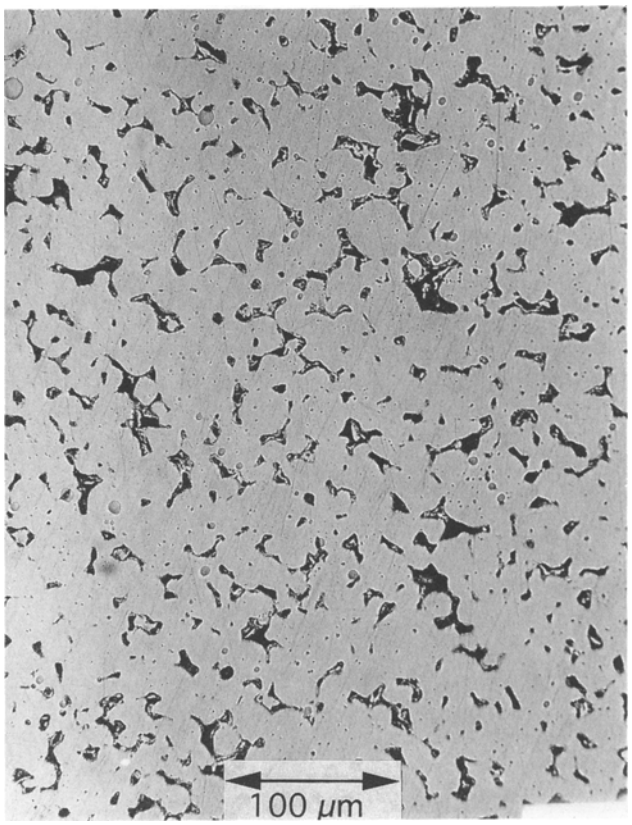

Fig. 9 Sintered microstructure of vacuum-Ar debinding atmospheres at the center

Density measurements of debound samples determined by ASTM B328-73 (Ref 6) indicated 70.4 to 72.9% of theoretical density and interconnected porosity ranging from 18.4 to 24.5 vol % . Figure 5 plots density and interconnected porosity for debinding conditions (Ar, vacuum, air). Interconnected porosity levels were 24.5% for argon, 21.6% for vacuum, and 18.4% for air. These results are good indicators of an established interconnected network of porosity in the sample. For this reason, the remaining binder in all three atmospheres can be decomposed rapidly due to the high permeability of the sample (Ref 7). The porosity will also allow oxygen to react with the residual carbon. The density, as a percentage of theoretical, was about 71% for argon, 70% for vacuum, and 73% for air. The densities of the samples from the argon and vacuum are nearly the same as the original powder loading. The density of the samples from the air debound samples indicate that residual binder; binder decomposition products or oxide was still in the powder matrix. The high level of residual contaminants hindered final stage debinding and densification during sintering.

3.2 *Final Stage Debinding and Sintering*

Samples exposed to the O_2/Ar mixture during final stage debinding exhibited brighter color and sheen. Density and interconnected porosity were determined using ASTM B328-73 and are plotted in Fig. 5. The highest densities and lowest interconnected porosity were obtained using Ar-O_2/Ar, Ar-Ar, and vacuum-O_2/Ar atmospheres. See micrographs in Fig. 6 to 13. Figures 6 to 8 show a mixture of irregular pores and small round pores. Porosity was isolated, and the density was highest in these samples. Figure 9 shows lower levels of sintering and corresponds to higher interconnected porosity and lower density. Figure 10 shows similar sintering as in Fig. 6 to 8; however, there are prior particle boundaries evident indicating that contamination interfered with sintering. Figure 11 shows individual particles that did not sinter. Contamination in the pore volume interfered with sintering. This may be due to insufficient oxygen available to react with the carbon. Figures 12 and 13 are micrographs of the edges of the sample. In Fig. 12, the surface sintered well and is similar to the center section in Fig. 7. Figure 13 shows poor sintering on the edge indicating that contamination that was not removed prevented sintering on the edge. A comparison of the edge of the sample in Fig. 11 and the center of the sample in Fig. 10 indicates that this edge was in contact with the supporting substrate and did not receive sufficient exposure to the process gasses.

Chemistry is summarized in Table 4. Carbon was successfully controlled with all of the oxidizing atmospheres. The Ar-O_2/Ar atmosphere had the lowest value for carbon and corresponded with the lowest oxygen levels and highest density. Air treatment had the highest levels of oxygen, which corresponded to the lowest densities.

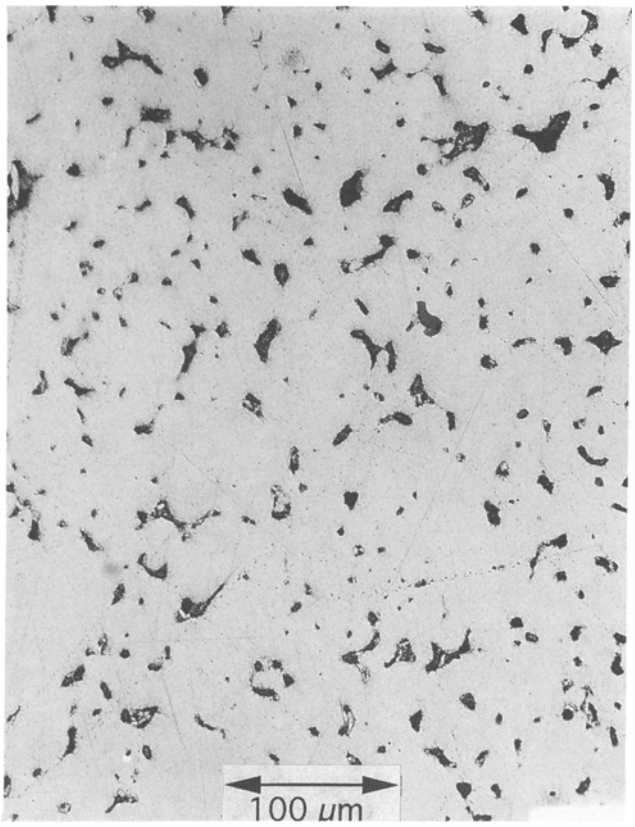

Fig. 10 Sintered microstructure air-Ar debinding atmospheres at the center

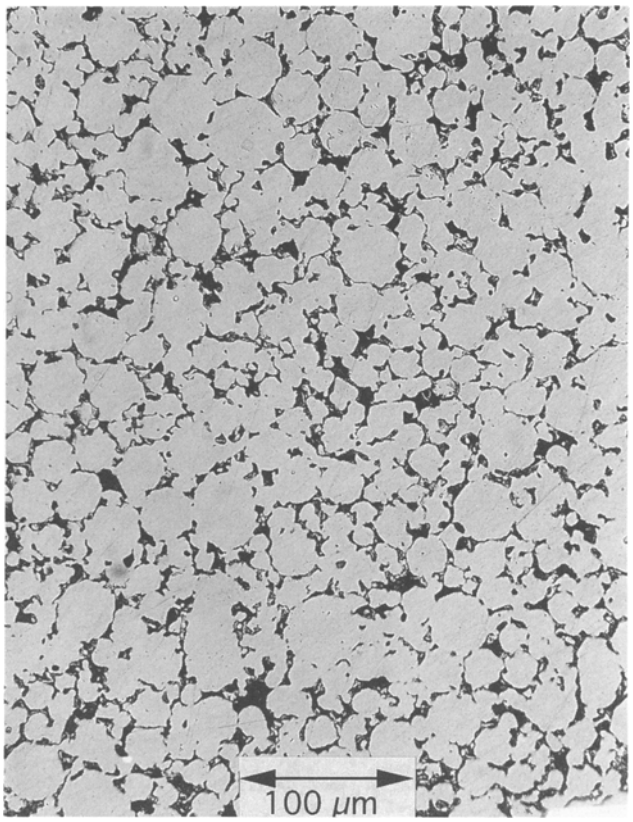

Fig. 11 Sintered microstructure air-O_2/Ar debinding atmospheres at the center

Table 4 Results of carbon and oxygen analysis of sintered samples by inert gas fusion

Atmosphere history		Carbon,	Oxygen,
First stage	Final stage	wt ppm	wt ppm
Air	O_2/argon	32-34	911-3030
Air	Argon	27-32	272-946
Argon	O_2/argon	17-18	126-177
Argon	Argon	118	196-217
Vacuum	O_2/argon	55	454-492
Vacuum	Argon	192 to 195	484-730

Nitrogen was also analyzed for the processed samples. Nitrogen ranged from a maximum of 50 ppm by weight in the vacuum-argon sample to a minimum of 30 ppm by weight in the air-argon and argon-argon atmospheres. This indicates that nitrogen in the processing atmosphere did not significantly affect the chemistry of the sintered sample.

Figures 14 and 15 plot dimensional changes for the samples processed in each atmosphere. First stage debinding, Fig. 14, resulted in dimensional changes of less than one percent except for one value of 1.1% for the thickness in the air debound samples. Vacuum debinding shows less spread from maximum to minimum on the diameter and thickness than the other atmospheres. This may indicate better dimensional control using vacuum to remove low temperature components from the compact. Argon atmospheres indicate that slumping likely occurred due to general increase in diameter and decrease in thickness. Air debinding indicates that dilation likely occurred due to general decrease in diameter and an increase in thickness. Dimensional change from molded to sintered, Fig. 15, indicated close data spread from maximum to minimum values in the vacuum and argon first stage atmospheres. This indicates good dimensional control and corresponds to the highest densities. The samples exposed to air processing showed more spread, probably caused by uncontrolled first stage debinding.

4. Discussion

Air used in first stage debinding introduced excess oxygen during debinding, caused combustion, and likely formed complex hydrocarbon species that did not decompose as readily as the original binder. Combustion also caused excessive pressure buildup in the samples creating defects and unacceptable dimensional control. Lower densities resulted from two sources: swelling of the compact and trapped contamination in the compact.

Argon used as the first stage debinding atmosphere resulted in controlled decomposition of the binder as evidenced by TGA and DTA. Slumping of the samples may have been caused by high partial pressures of volatilized binder species in the sample region; this allows condensation to occur on or near the sur-

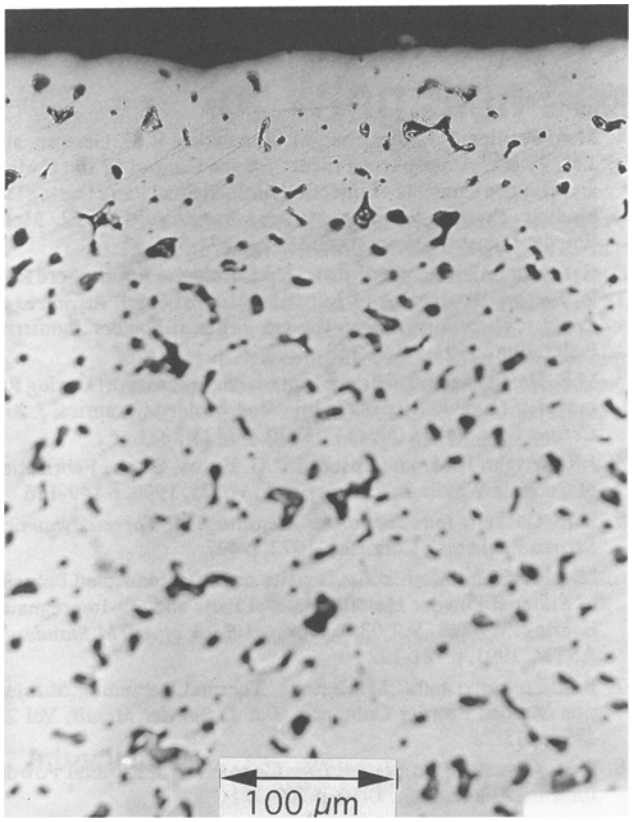

Fig. 12 Sintered microstructure Ar-O_2/Ar debinding atmospheres at the edge

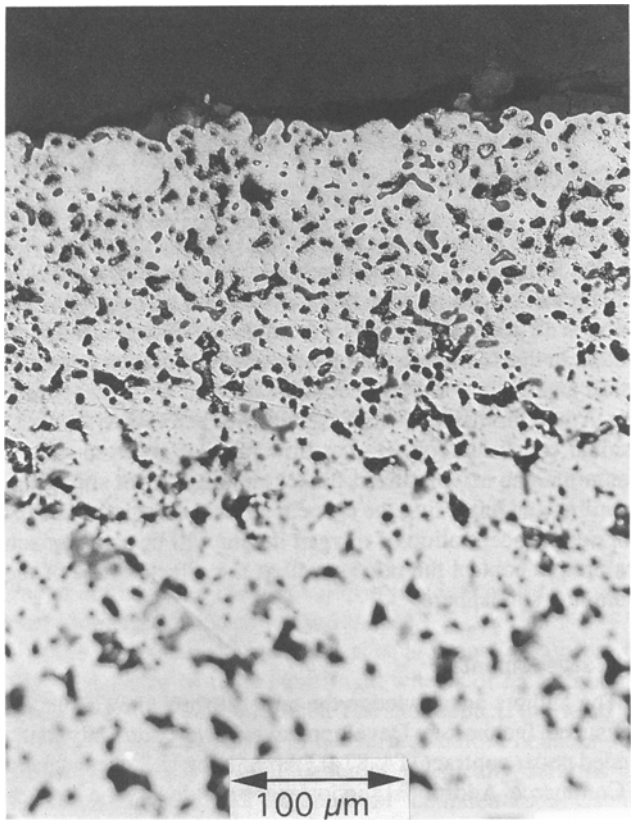

Fig. 13 Sintered microstructure of air-Ar debinding atmospheres at the edge

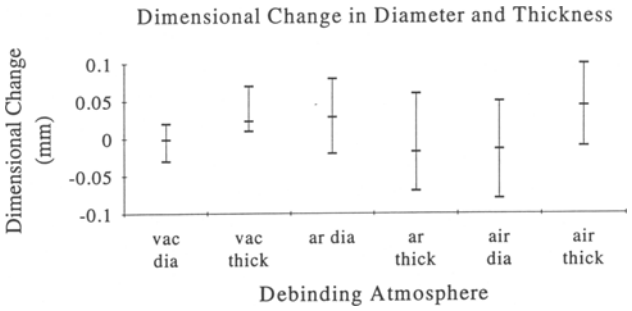

Fig. 14 Dimensional changes in diameter and thickness, maximum, minimum, and average values, of samples from as molded to first stage debinding

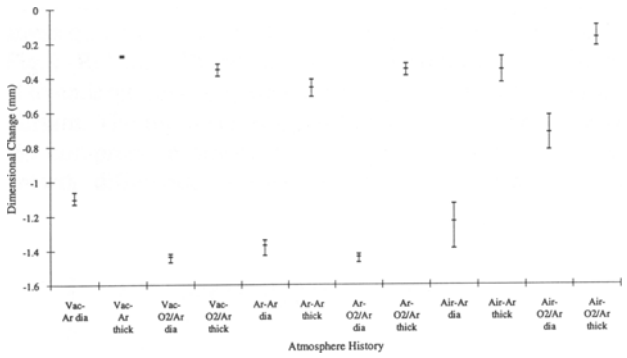

Fig. 15 Dimensional changes in diameter and thickness, maximum, minimum, and average values, as molded to sintered

face of the sample. The liquid volume near the surface increases, either by vapor condensation and by liquid transported from the interior of the sample by capillary attraction. As binder accumulates, the contact angle between the binder and the powder particles increases. Large contact angles create repulsive forces, and small contact angles create attractive forces. The compact will expand due to an increase in repulsive forces as the contact angle between the particles and liquid binder increases relative to the liquid volume (Ref 8). This will cause the particles to separate creating an unstable structure allowing gravity to overcome the frictional forces between particles. Dimensional data indicated that slumping occurred. Argon atmosphere in first stage debinding lowered levels of carbon and maintained oxygen contamination within reasonable levels. Oxygen and carbon levels in the Ar-O_2/Ar debinding atmosphere were the lowest of all of the atmospheres.

Vacuum debinding resulted in good dimensional control probably due to lowering the vapor pressure of the binder in the furnace and allowing the binder to volatilize at lower temperature. There was benefit in using O_2/Ar during final stage debinding in removing carbon. Oxygen was not controlled as well

as in the argon first stage debinding atmosphere. Possibly there was sufficient partial pressure of oxygen in the vacuum furnace to oxidize the copper powder. Density was improved by using an O_2/Ar atmosphere during final stage debinding.

5. Conclusions

Debinding atmosphere affected final sample chemistry and density. Removal of carbon resulting from the decomposition of hydrocarbon binders can be accomplished by controlled reaction with partial pressures of oxygen. Controlled oxygen content in the debinding atmosphere reduced carbon contamination and limited oxygen contamination in the copper samples. Argon produced the highest densities and lowest levels of residual contamination. Higher flow rates of argon to reduce accumulations of volatilized binder should control slumping. Sampling and analyzing the effluent gas and calculating an appropriate concentration of oxygen in situ will be an approach explored to control the rate as well as the effectiveness of the debinding atmosphere.

Acknowledgments

The authors acknowledge the support from the Center for Advanced Technology Development at Iowa State University, funded under contract ITA-87-02 through the U.S. Department of Commerce. Additional support was provided by the Department of Energy USDOE/BES-Materials Science Division under Contract W-7405-ENG-82.

References

1. M.A. Phillips, E.L. Streicher, M. Renowden, R.M. German, and J.M. Friedt, Atmosphere Process for the Control of the Carbon and Oxygen Contents of Injection Molded Steel Parts During Debinding, *Powder Injection Molding Symposium—1992*, Metal Powder Industries Federation, 1992, p 371-384
2. E. Streicher, M. Renowden, and R.M. German, Atmosphere Role in Thermal Processing of Injection Molded Steel, *Advances in Powder Metallurgy—1991 Volume 2*, Metal Powder Industries Federation, 1991, p 141-158
3. M.R. Barone and J.C. Ulicny, Liquid-Phase Transport During Removal of Organic Binders in Injection-Molded Ceramics, *J. Am. Ceram. Soc.*, Vol 73 (No. 11), 1990, p 3323-3333
4. J.K. Wright, R.M. Thompson, J.R.G. Evans, On the Fabrication of Ceramic Windings, *J. Mater. Sci.*, Vol 25, 1990, p 149-156
5. D.R. Gaskell, *Introduction to Metallurgical Thermodynamics*, Scripta Publishing Company, 1973, p 497
6. "Standard Test Method for Density and Interconnected Porosity of Sintered Powder Metal Structural Parts and Oil-Impregnated Bearings," B328, Vol 02.05, *Annual Book of ASTM Standards*, ASTM, 1991, p 121-122
7. B.K. Lograsso and R.M. German, Thermal Debinding of Injection Molded Powder Compacts, *Int. J. Powder Metall*, Vol 22, 1990, p17-22.
8. R.M. German, *Particle Packing Characteristics*, Metal Powder Industries Federation, 1989, p 309-351